AUTOMATED EXTRACTION OF PROFILES FROM 3D-MODELS OF ARCHAEOLOGICAL FRAGMENTS

H. Mara and M. Kampel
Pattern Recognition and Image Processing Group, Institute for Automation, Vienna University of Technology,
Favoritenstraße 9/1832, A-1040 Vienna, Austria, Fax: +43(1)58801-18392
e-mail: {mara, kampel}@prip.tuwien.ac.at

KEY WORDS: Cultural Heritage, Automation, Development, Processing, Reconstruction, Profile-Line, Pottery.

ABSTRACT

Motivated by the requirements of the present archaeology, we have been developing an automated archivation system for archaeological classification and reconstruction of ceramics. Our system works with the profile of an archaeological fragment, which is the cross-section of the fragment in the direction of the rotational axis of symmetry. Ceramic fragments are recorded automatically by a 3D-measurement system based on structured light. The input data for the estimation of the profile is a set of points produced by the acquisition system. The profile is used to reconstruct the original pot.
Our approach consists of several steps, starting by calculating the proper orientation, which describes the exact positioning of the fragment on the original vessel. Next the profile line is computed and several measurements, like the diameter and height of the vessel. After evaluating the profile line a virtual pot is reconstructed.
The performance of the proposed algorithm was tested on real data and the results are presented in this paper.

1 INTRODUCTION

Today's archaeology requires the storage, reconstruction and classification of ceramics, which is done manually. So we were motivated to develop an automated system, which meets the requirements for automation. A large number of ceramic fragments, called sherds, are found at every excavation site (Figure 1). The physical characteristics of archaeological pottery are used in archaeometry (Leute, 1987) to assess cultural groups, population movements, inter-regional contacts, production contexts, and technical or functional constraints. Therefore an analytical tool with a defined methodology is required for classification of artifacts (Orton et al., 1993).

Fragments are documented by being photographed, measured, and drawn; then they are classified. The purpose of *classification* is to get a systematic view on the excavation finds.

Figure 1: Boxes filled with ceramics stored in archives.

Traditional archaeological classification is based on the so-called profile of the object, which is the cross-section of the fragment in the direction of the rotational axis of symmetry. This profile line has to be the longest elongation around a sherd parallel to its rotational axis. A two-dimensional plot of the profile line holds all the information needed to perform archaeological research. The correct profile and the correct axis of rotation are thus essential to reconstruct and classify archaeological ceramics.

Archaeologists use characteristic points of the profile line and their distance ratios to determine which type of vessel a sherd belongs to (Orton et al., 1993). Figure 2 shows the characteristic points of a manual drawn profile line of a complete object. The characteristic points shown are the inflection points (IP), local maxima (MA), local minima (MI), the outermost point, where the profile line touches the orifice plane (OP), the outermost point, where the profile line touches the base plane (BP) and the point, where the profile line touches the axis of rotation. A detailed set of rules for the classification based on the characteristic points was discussed in (Mara et al., 2002).

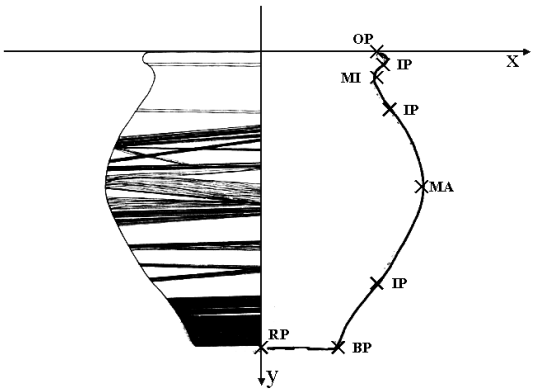

Figure 2: Manual drawing of a pot, with manually estimated characteristic points

The next Section describes the processing of the data starting with the acquisition of the 3D-data. Then the profile line and its estimation using the rotational axis is described. In Section 3 experiments and results based on real data-sets, are shown. Finally an outlook for future work is presented.

2 DATA PROCESSING

In earlier work (Adler et al., 2001) a scanning technology was described, which directly acquired the profile line by projecting a laser-line on the sherd. This laserline was captured by a camera for the inner side and a second camera for the outer side. The merged images of these two cameras contained the profile line. This system had drawbacks concerning its portability, ease of use and automation. Therefore we choose the *Eyetronics ShapeSnatcher Technology* (Cosmas et al., 2001) (see Figure 3), because it is portable and can be operated without expert knowledge. It consists of a CCD-camera and a flashlight to acquire the shape based on the structured light principle. The image, together with the knowledge about the pattern and its relative position to the camera, are used to calculate the coordinates of points belonging to the surface of the object (Kampel and Sablatnig, 1999). Since the 3D-scanner can only capture one side of the sherd per scan, the inner side and the outer side have to be scanned separately to reconstruct a complete 3D-model of the sherd.

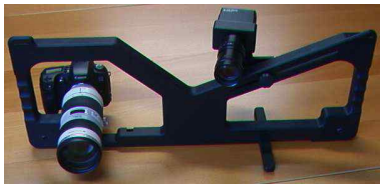

Figure 3: Eyetronic's ShapeCam consisting of a CCD-camera (left) and a flashlight mounted on the top-right part of the handling frame.

2.1 3D Data - VRML

The 3D-data acquired by the 3D-scanner is stored as 3D-surface, which consists of 3D-points (vertices) that are connected in form of triangles (called faces). The 3D-model contains the color information (called texture) for each face for visualization. These vertices and faces are stored in an indexed list ($\mathcal{L}$).

There are different types of file formats for storing 3D-data (e.g. AutoCAD, Wavefront, OpenInventor). We have chosen VRML (Nadeau, 1999), which is software independent and can be viewed with a web-browser with a VRML-plugin that is free of charge.

The pottery data set we use for experiments consists out of the recorded objects described in table 1. The number of pieces per view is 2, because for every piece an inner view and an outer view has been acquired.

For storage in a database we use polygonal geometrical objects (Nadeau, 1999). These geometrical objects are described by an indexed list $\mathcal{L}_v$ of n vertices $\mathbf{p}_i = (x_i, y_i, z_i)^T$. x_i ,y_i and z_i are the coordinates of the vertices of the surface of the object in centimeter.

	Box 1	Box 2	Box 3
Number of pieces	21	12	26
Number of views/piece	2	2	2
Vertices/View	4.000-9.000		3.000-8.000

Table 1: MURALE Pottery dataset

$$\mathcal{L}_v = \{\mathbf{p}_1, \ldots, \mathbf{p}_{k_1}, \ldots, \mathbf{p}_{k_2}, \ldots, \mathbf{p}_{k_3}, \ldots, \mathbf{p}_n\} \quad (1)$$

The vertices of $\mathcal{L}_v$ are connected by faces f, which are stored as list $\mathcal{L}_f$.

$$\mathcal{L}_f = \{f_1, \ldots, f_m\}, f_k = (k_1, k_2, k_3) \quad (2)$$

Optionally the normal vectors $\mathcal{L}_n = \{\mathbf{n}_1, \ldots, \mathbf{n}_n\}$ and the color information $\mathcal{L}_c = \{c_1, \ldots, c_n\}$, $c_i = (\textit{red}, \textit{green}, \textit{blue})$ is stored, which is not necessary for further calculation, but it is used for visualization purposes. The normal vectors $\mathcal{L}_n$ are used for the estimation of the rotational axis. If they are not provided by the scanning software, they are estimated by using the triangulated data.

So the 3D-model of the view is described by an indexed list of vertices, faces, normal vectors and color information: $\textit{sherd}_{\textit{view}} = \{\mathcal{L}_v, \mathcal{L}_f, \mathcal{L}_n, \mathcal{L}_c\}$.

To double the performance of processing the data, we use two different types of coordinate systems. For translation and rotation we use the cartesian coordinate system, because the translation is done by an addition. To estimate the two angles (azimuth and elevation), which is required for rotation we use a spherical coordinate system. Points $\mathbf{p}$ and vectors $\mathbf{v}$ in $\mathbb{R}3$ using the spheric representation are described by the azimuth θ, elevation ϕ and the distance r to the origin point in the cartesian coordinate system. This representation has been chosen for the rotation, because rotation can be done by an addition. Cartesian $\mathbf{p}_{=}(x, y, z)^T$ and spheric: $\mathbf{p}_{=}(\theta, \phi, r)^T$ notation.

2.2 Profile line

The rotational axis *rot* leads to the exact position of a fragment on the original vessel. Therefore the rotational axis is required for the estimation of the profile line and for registration (Sablatnig and Kampel, 2002) of the inner and outer view.

The profile line, which is used by archaeologists for classification and reconstruction, is defined below:

- A profile line (*profile*) is the cross-section of the 3D-model of the sherd (*sherd*) and an intersecting plane e_i. This intersecting plane e_i, is defined by *rot* and the direction i, so that e_i intersects the *sherd*.
- The intersection at an index i_{max}, where the sherd has the maximum height $h_{max} = max(h_i)$ is the profile line with the longest arc length and is called longest profile line ($\textit{profile}_{max}$). The index specifies the direction.
- The height h_i is defined as distance between two points of the surface of the sherd parallel to the rotational axis *rot*. The index i, where the height has its maximum is called h_{max}.

A sherd, its rotational axis and the estimated longest profile line is shown in Figure 4.

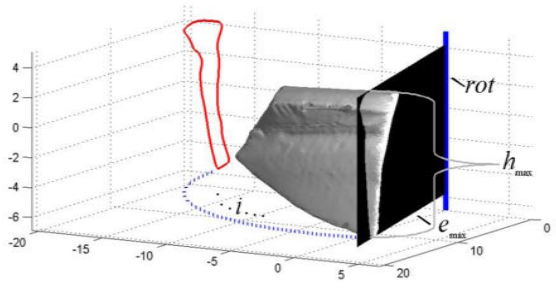

Figure 4: Oriented sherd, rotational axis *rot*, intersecting plane e_i, longest profile line $profile_{max}$, h_{max}

2.3 Estimation of the Profile Line

For the extraction of the profile line all vertices that are connected by an edge of the face intersecting the plane e_i are selected. Therefore the Hessian normal form $ax^2 + by^2 + cz^2 + d = 0$ is used to determine the distance d to the plane. The sign of the distance and the relative distance with respect to the maximum distance is used to reduce the number of vertices for the estimation of the profile line. Vertices with a $d < 0$ are located on the left side of the plane. Vertices with $d > 0$ are located on the right side. Every face consists of three or more vertices, where each pair of vertices describe an edge of the face (see figure 5). The pairs of vertices, with vertices on different sides of the intersecting plane e_i are used to estimate the points of intersection of the edges and the intersecting plane e_i, because the vertices of the 3D-model need not be located on the e_i. The result of connection of the points of intersection is the profile line.

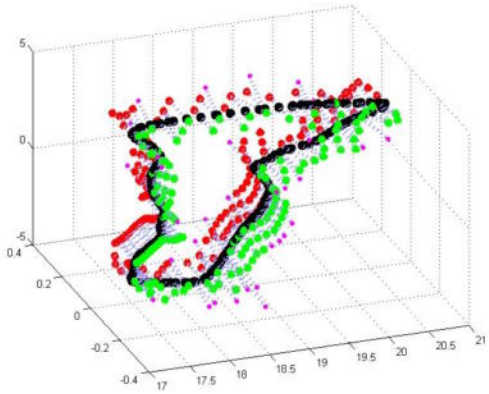

Figure 5: Vertices $\mathbf{p}_{d<0.01}$ left (light gray) and right (dark gray) of the intersecting plane, edges $edge_{intersect}$, vertices of the profile line $\mathbf{p}_{intersect}$ (black).

- First the relative distance (shown in Figure 6 as gray - value) with respect to the maximum distance between the vertices and the xz-plane is estimated. Experiments have shown that vertices with a distance larger than 1% can not be used for the estimation of the profile line, because the edges, they belong to do not intersect e_i. This threshold depends on the resolution of the 3D-scanner and can be adjusted, when another resolution is used.

- In the next step the faces $f_{d<0.01}$, which contain the indices of the nearest vertices $\mathbf{p}_{d<0.01}$ are selected. These faces $f_{d<0.01}$ are split into edges, for estimation of the vertices of the profile line: A $f = \{i, j, k\}$ connects the vertices $\mathbf{p}_i$, $\mathbf{p}_j$ and $\mathbf{p}_k$, so the edges of the face f are described by $edge = \{(i, j), (j, k), (k, i)\}$. Each of these vertices can have a positive or a negative sign, which corresponds to the position with respect to intersecting plane. A vertex with a negative sign is located on the left side and a vertex with a positive sign is located on the right side of the plane. So the edges $edge_{intersect}$, which intersect the plane e_i must contain one vertex with a negative sign and one with a positive sign. The points from those edges $edge_{intersect}$ $\mathbf{p}_{intersect}$ are selected and the parameters of the line describing these edges $edge_{intersect}$ are estimated. With these parameters the point of intersection $\mathbf{p}_{intersect}$ between the line and the intersecting plane (equal to the xz-plane) is estimated. These points $\mathbf{p}_{intersect}$ are connected with their nearest neighbor. They define the profile line $profile$.

- All vertices $\mathbf{p}_{intersect}$ of the profile have the distance $y = 0$ to the intersecting xz-plane. The x-coordinate is the distance (radius r) to the rotational axis *rot* and the z-coordinate is the height h (see Equation 3).

$$profile = \{..., (x_i, 0, z_i)^T, ...\} \rightarrow \{..., (r_i, h_i)^T, ...\} \quad (3)$$

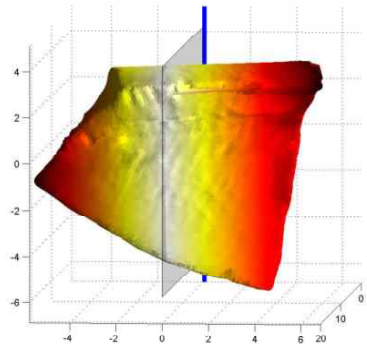

Figure 6: Oriented sherd and intersecting plane e_i. The level of gray of the surface of the sherd corresponds to the distance of its vertices $\mathbf{p}$ to e_i. Lighter means nearer.

2.4 Longest profile line

For classification and reconstruction only the longest profile line is used. In this procedure multiple profile lines are extracted and the longest is selected for further processing. All profile lines are used to evaluate the estimation of the rotational axis and the registration of the inner and outer view (see Section 3).

The number of profiles, which are extracted depends on the resolution of the 3D-scanner and the size of the sherd. Experiments have shown that 12 extracted profiles have the best ratio between performance and accuracy. In Figure 7 four multiple intersecting planes e_i are shown as light gray rectangles aligned along the rotational axis. The rotational axis is shown as vertical black line starting at the point of origin. The gray object is the 3D-model of the sherd and the black lines around this model are the intersection between the sherd and the planes e_i, representing multiple profile lines $profile_i$. Instead of estimating the distance d for

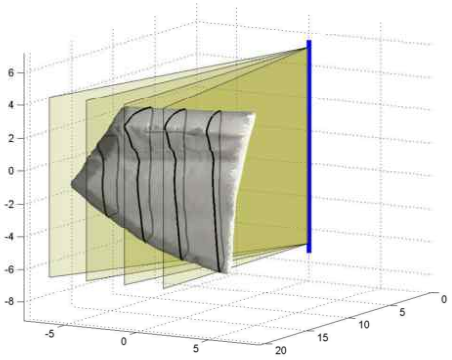

Figure 7: Sample of intersecting planes e_i

each vertex to an intersecting plane e_i, the sherd is rotated so that the intersecting plane is the xz-plane. Afterwards the y-coordinate is the distance d to the intersecting plane. Experiments have shown that the rotation is ten times faster than using the Hessian normal form, because a single matrix multiplication for the rotation is done faster than a loop of multiplications and additions with $MATLAB$.

The sherd has to be rotated 12 times by γ_i (see Equation 4).

$$\gamma_i = \frac{max(\mathcal{L}_v(\theta)) - min(\mathcal{L}_v(\theta))}{n}, \text{ i.e.} n = 12 \quad (4)$$

As the rotational axis is identical to the z-axis the rotation is done by using $\mathbf{R}_z(\gamma)$. This rotation positions the sherd so that the intersecting plane e_i is the xz-plane. After this rotation the distance for every vertex at every intersection is equal to the y-coordinate of each vertex. After every rotation a profile line is extracted and the arc length is estimated. Afterwards the arc length is estimated and the profile with the longest arc length is selected.

3 EXPERIMENTS

For evaluation of the estimation of the rotational axis the mean diameter for each profile is estimated. If the standard deviation of these mean diameters exceeds a certain threshold given by archaeologists (i.e. $0.5\ cm$) the estimation of the rotational axis was not correct. Extracted multiple profiles based on a correct estimated rotational axis are shown in Figure 8a. The multiple profile lines have similar shape and position with respect to variations of the surface and the breakage. In Figure 8b the rotational axis was not estimated correctly, because the fragment was to flat. The y-axis in both figures shows the radius in cm and the x-axis shows the height in cm. For the evaluation of

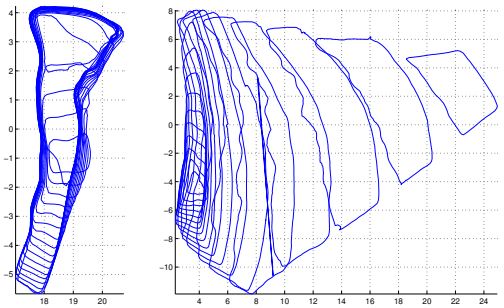

(a) (b)

Figure 8: (a) Multiple profile lines using a correct estimated rotational axis (b) Multiple profile lines using an incorrect rotational axis

the registration the minimum and maximum radius of each profile is estimated in addition to the registration error defined in (Sablatnig and Kampel, 2002). In case of pottery the radius is measured as the orthogonal distance between the rotational axis and a point of the sherd. The difference between the minimum and maximum radius is the thickness of the sherd. As the range of the thickness of a sherd is known a priori, a lower threshold (e.g. $0.5\ cm$) and an upper threshold (e.g. $2\ cm$) can be set. These two thresholds depend on the material used and the manufacturing process and are given by archaeologists. The radius and the standard deviation of the mean radius of the profiles from Figure 8a and Figure 8b are shown in Figure 9a and Figure 9b. The x-axis in Figure 9 shows the elevation θ in degree and the y-axis the z-normalized diameter in centimeter.

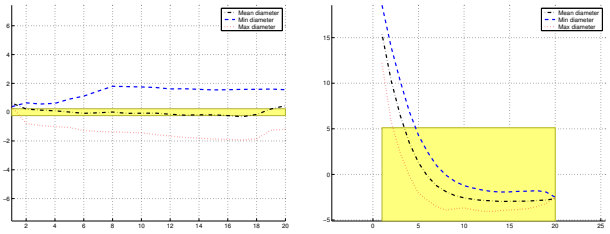

(a) (b)

Figure 9: Maximum, mean and minimum radius.

3.1 Reconstruction of the Pot

For the reconstruction the vertices $\mathbf{p}_{profile_{max}}$, which define the longest profile line, are copied n times. Each copy $\mathbf{p}_{profile_{max_n}}$ of the vertices of the longest profile is rotated, using $\mathbf{R}_z(n*\pi/180)$. The faces of the reconstructed object are estimated by connecting each point $\mathbf{p}_m$ with its neighbors to quadrangular mesh. Quadrangles have been chosen, because of the arrangement of the neighboring points to each other:

Let k be the number of vertices of the profile line, than the indices of the neighbors of $\mathbf{p}_m$ are: $m+1$, $m+k$ and $m+k+1$.

The smoothness of the visualization of the reconstructed 3D-model depends on n. Larger n means smoother, but slower to display. Experiments have shown that $180 < n < 360$ is the best trade off between performance and quality of the visualization of the reconstructed object.

Reconstruction is done by rotating the *profile* 360° about the rotational axis using $\mathbf{R}_z(\gamma)$.

$$\begin{aligned} object &= \{profile * \mathbf{R}_z(\gamma_i)\},\ i = 1 \ldots n, \\ \gamma_1 &= 0,\ \gamma_{i+1} = \gamma_i + \Delta\gamma,\ \Delta\gamma = 2 * \pi / n \end{aligned} \quad (5)$$

Figure 10a shows the reconstruction of a pot and Figure 10b shows the reconstruction of fragment. The reconstruction of these two Figures were based on the longest profile line from Figure 8.

4 RESULTS

Experiments were done on the 33 sets of 3D images stored in box 1 and 2 and 26 real data sets from box 3 of archaeological fragments given by archaeologists for testing. Each set contained one image of the inner half and one of the outer half of the sherd. In 29% of the sherds the estimation of the rotational axis returned a correct result. 31% of the results had two different types of minor errors, which are still acceptable for further processing.

The first acceptable error was a to large distance between the inner and out half (2 to 3 cm). The second acceptable error was a slightly twisted (less than 10°) inner half compared to the orientation of the outer half. These two errors have been observed on small sherds or sherds with a small curvature (Sablatnig and Kampel, 2002). For 7 sets the estimation of the rotational axis did not have a correct result, because the sherd were to small, to flat, contained a handle or were part of a bottom fragment. All of these 7 sets have normal vectors, which do not point at the rotational axis. So the estimation of the rotational axis was not done correctly.

The success rate for correct extraction of the profile line and consequently the percentage of sherds, which is used for further classification is 50% of the sherds found at the excavation site. This has to be seen with respect to manual archivation done by archaeologists (Orton et al., 1993): for coarse ware 35% (Degeest, 2000) and for fine ware 50% (Poblome, 1999) of the findings are used for further classification. It depends on the ratio between bending of the curvature (Matas et al., 1995, Bennett and MacDonald, 1975) and the fragment and its diameter (Sablatnig and Kampel, 2002) (e.g. handle, flat fragments like bottom pieces, small size, etc.).

The execution time using a prototype written in $MATLAB$ running on a $Pentium\ III$ 1 GHz is less than a minute per sherd. The estimation of *rot* takes 70% to 80% of the execution time for processing one sherd described by the inner and outer view. Comparing the execution time for the extraction and segmentation of profile lines to the time used by archaeologists drawing a profile line by hand shows that the number of classification per day can be increased dramatically.

The estimation of the rotational axis will also be used to reconstruct whole objects from several sherds. Figure 10a displays a reconstructed pot (gray object) out of one fragment (dark object) based on the profile line (light line) and its axis of rotation (dashed line). Figure 10b shows a detailed part of the same object as Figure 10a. Table 2

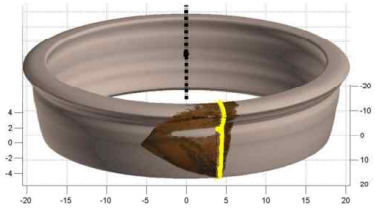

(a)

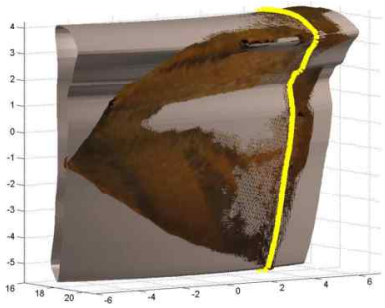

(b)

Figure 10: (a) Reconstructed (gray) pot and (b) fragment, cross-section (light gray line), recorded fragment (dark gray) and its rotational axis (vertical dashed line).

shows successfully estimated features for further classification of box 1 and box 2. These features are the diameter at the highest point of the sherd (rim-diameter rdm in cm). The maximum diameter of the sherd orthogonal to the rotational axis (wall-diameter wdm in cm). The diameter at the lowest point of the sherd (bottom-diameter bdm in cm). The overall height (h_{max} in cm) of the sherd and the characteristic ratio $crat = h : rdm$. Box 3 contains

Box	Nr	rdm	wdm	bdm	h_{max}	$crat$
1	04	25,16	75,61	24,94	7,12	0,33
1	08	31,78	50,16	32,08	5,63	0,63
1	16	30,68	49,32	30,9	6,68	0,62
1	17	32,64	42,31	34,32	8,81	0,77
1	18	32,34	31,06	32,1	4,68	1,04
1	19	28,9	33,80	29,38	9,15	0,85
1	20	26,78	30,15	27,32	7,09	0,89
1	22	22,8	27,62	23,86	6,04	0,83
1	23	24,58	44,61	25,32	7,4	0,55
2	01	20,68	54,22	20,8	7,05	0,38
2	02	32,58	35,02	32,9	8,94	0,93
2	04	12,54	35,66	17,38	6,9	0,35
2	05	19,92	25,79	20,56	6,15	0,77
2	06	6,84	22,85	7	10,15	0,30
2	09	24,66	19,05	25,76	6,96	1,29

Table 2: Results of proper registered and orientated sherds.

sherds with handles and sherds with a large curvature with respect to box 1 and box 2. Experiments have shown that the extraction of the profile line could be done on 5 out of 26 sherds of box 3. Figure 11 shows a sherd containing a handle, where the estimated rotational axis is incorrect.

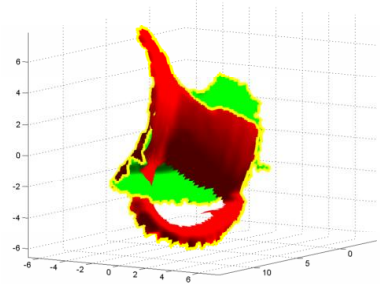

Figure 11: Piece 8 from box 3 registered using an incorrect estimated rotational axis. The dark gray part is the outer view containing the handle. The light gray part is the inner view of the sherd.

5 CONCLUSION AND OUTLOOK

We have proposed an automated system for extraction of the profile line, which was required for archaeological classification and reconstruction. The work is part of a documentation system for ceramics. The acquired 3D-views have been registered and oriented using the rotational axis. Afterwards the profile line was extracted by intersecting planes from the registered and orientated 3D-views of the sherd. The method has been tested on real data with reasonable good results. Also sherds that can not be processed manually, because of their low curvature, can be processed by the presented system.

Future work will go towards making the existing system more robust with respect to the sherds with handles and bottom fragments, so that the registration can be applied on a larger percentage of sherds. The presented system is able to determine, when the estimation of the rotational axis fails, but it can not detected the reason (e.g. handle) for that. So a detection and separate processing of sherd with handles or bottom-pieces would increase the performance of the system.

As the rotational axis leads to the position of the fragment in the unbroken vessel multiple fragments will be matched to reconstruct the whole object. Figure 12 shows a whole object, which was reconstructed manually by archaeologists. This could be done by matching the profile lines from different sherds of one object, so that the whole object can be reconstructed.

ACKNOWLEDGEMENTS

This work was partly supported by the Austrian Science Foundation (FWF) under grant P13385-INF, the European Union under grant IST-1999-20273 , the Austrian Federal Ministry of Education, Science and Culture and by the innovative project ’3D technology’ of the Vienna University of Technology.

Figure 12: Complete manually reconstructed vessel.

REFERENCES

Adler, K., Kampel, M., Kastler, R., Penz, M., Sablatnig, R. and Hlavackova-Schindler, K., 2001. Computer aided classification of ceramics - achievements and problems. In: W. Börner and L. Dollhofer (eds), Proc. of 6th Intl. Workshop on Archaeology and Computers, Vienna, Austria, pp. 3–12.

Bennett, J. and MacDonald, J., 1975. On the Measurement of Curvature in a Quantized Environment. IEEE Trans. on Computer 24, pp. 803–820.

Cosmas, J., Itagaki, T., Green, D., Grabczewski, E., Gool, L. V., Zalesny, A., Vanrintel, D., Leberl, F., Grabner, M., Schindler, K., Karner, K., Gervautz, M., Hynst, S., Waelkens, M., Pollefeys, M., DeGeest, R., Sablatnig, R. and Kampel, M., 2001. 3D MURALE: A multimedia system for archaeology. In: Proc. of Intl. EuroConference on Virtual Reality, Archaeology and Cultural Heritage, Athens, Greece, pp. 297–305.

Degeest, R., 2000. The Common Wares of Sagalassos. In: M. Walken (ed.), Studies in Eastern Mediterranean Archaeology, III.

Kampel, M. and Sablatnig, R., 1999. On 3D modelling of archaeological sherds. In: Proceedings of International Workshop on Synthetic-Natural Hybrid Coding and Three Dimensional Imaging, Santorini, Greece, pp. 95–98.

Leute, U., 1987. Archaeometry: An Introduction to Physical Methods in Archaeology and the History of Art. John Wiley & Sons.

Mara, H., Kampel, M. and Sablatnig, R., 2002. Preprocessing of 3D-Data for Classification of Archaelogical Fragments in an Automated System. In: F. Leberl and F. Frauendorfer (eds), 26th Workshop of the Austrian Association for Pattern Recognition (OeAGM/AAPR), Graz, Austria, pp. 257–264.

Matas, J., Shao, Z. and Kittler, J., 1995. Estimation of Curvature and Tangent Direction by Median Filtered Differencing. In: 8th International Conference on Image Analysis and Processing, pp. 83–88.

Nadeau, D., 1999. Building virtual worlds with vrml. In: Computer Graphics and Applications, IEEE, pp. 18–29.

Orton, C., Tyers, P. and Vince, A., 1993. Pottery in Archaeology. Cambride University Press.

Poblome, J., 1999. Sagalassos Red Slip Ware. In: M. Walkens (ed.), Studies in Eastern Mediterranean Archaeology, II, Brepols.

Sablatnig, R. and Kampel, M., 2002. Model-based registration of front- and backviews. Computer Vision and Image Understanding 87(1–3), pp. 90–103.